Photo-Plasmonic Effect as the Hot Electron Generation Mechanism

M. Akbari-Moghanjoughi (massoud2002@yahoo.com)
Azarbaijan Shahid Madani University

Article

Keywords:

Posted Date: September 28th, 2022

DOI: https://doi.org/10.21203/rs.3.rs-2094148/v1

Photo-Plasmonic Effect as the Hot Electron Generation Mechanism

M. Akbari-Moghanjoughi

Faculty of Sciences, Department of Physics,

Azarbaijan Shahid Madani University,

51745-406 Tabriz, Iran

massoud2002@yahoo.com

(Dated: September 23, 2022)

Abstract

Based on the effective Schrödinger-Poisson model a new physical mechanism for resonant hot-electron generation in half-space metal-vacuum configuration of electron gas with arbitrary degree of degeneracy is proposed. The energy dispersion of undamped plasmons in the coupled Hermitian Schrödinger-Poisson system reveals an exceptional point coinciding the minimum energy of plasmon conduction band. Existence of such exceptional behavior is the well-know character of damped oscillation which in this case refers to resonant wave-particle interactions analogous to the collisionless Landau damping effect. The damped Schrödinger-Poisson system is used to model the collective electron tunneling into the vacuum. The damped plasmons is shown to have full-featured exceptional point energy dispersion phase diagram which can have many interesting technological applications. Depending on the tunneling parameter value, in the damped collective excitation band gap there are resonant energy orbital for which the wave-like growing of collective excitations cancels the damping due the quantum electron tunneling. This important feature is solely due to dual-tone wave-particle oscillation characteristics of the collective excitations in the quantum electron gas which leads to the resonant photo-plasmonic effect, as the plasmonic analog of the well-known photo-electric effect. The few nanometer wavelength high energy collective photo-electrons emanating from the typical metal surfaces lead to a much higher efficiency of plasmonic solar cell devices, as compared to their semiconductor counterparts base on electron-hole excitations at the Fermi energy level. The photo-plasmonic effect may be used to study the quantum electron tunneling and electron spill-out at metallic surfaces.

I. INTRODUCTION

Free electrons in metals and semiconductors control almost all fundamental physical properties of the solid [1]. Some basic properties of metals such as optical, electronic and thermodynamic ones are quite satisfactorily described by noninteracting electron (Drude) model [2]. The band structure model, on the other hand, has been a huge success and advancement in understanding of important quantum mechanical features of semiconductor material which was urgent for consequent development of the cutting edge nanoelectronic technology [3, 4]. There are of course some collective aspects of the electron gas with fundamental applications in plasmonics [5–7], optoelectronics [8, 9], nanotechnology [10] etc. which require advanced quantum many-body theories to cope with [11, 12]. Quantum electrodynamic [13], density function [14] and quantum hydrodynamic [15–21] theories have been some tools of the past solid state theory in order to descrobe collective physical behavior of quantum electron gas. Quantum fluid kinetic and hydrodynamic theories are however more common tools in the study of collective electronic (plasmon) excitations in complex plasmas where many other charged species and fields are involved. They are the results of many pioneering previous works in the field of collective quantum theory [22–38]. There has been some advancements in the hydrodynamic theories and their successful employment in various investigations of linear and nonlinear collective phenomena in dense degenerate plasmas involving both the laboratory scale phenomena [39–51] as well as the astrophysical plasmas [54–59]. One of derivatives of the quantum hydrodynamic theory is the effective Schrödinger-Poisson model [52] based on the pioneering Madelung quantum fluid theory [53]. The later model has shown some success in the study of key collective properties of the quantum electron gas, such as, generalized energy band structure [60], collective quantization of electron gas [61], collective effects on the electronic heat capacity in metals [62], the edge plasmon excitations and electron spill out effect [63], plasmon scattering [64], collective quantum interference [65], and more [66–68].

Plasmonics is one of the technologically appealing interdisciplinary active fields of physical sciences with a vigorous development over the past two decades [69, 70]. With turn of millennium the field has not fully achieved the desired pace in the rapidly growing semiconductor electronic industry of solar cell [71], sensors [72], modulators [73] and communications devices [74] for some definite reasons. Harvesting the collective electronic energy and their fast response in plasmonic devices requires inhibition of damping effects which is inherent in ordinary metals due to electron-phonon scattering and low mean free path collective response. However, while

the electron-electron scattering is greatly inhibited at quantum level due to the Pauli blocking mechanism, the only chance to reduce electron phonon scattering effect is a costly way of nanofabrication. Even in the absence of electron-ion collisions kinetic effects like collisionless Landau damping can greatly limit the plasmonic device operation. On the other hand quantum charge screening in metals blocks the collective response at low energy excitations. However, if the known technological obstacles is overcome, plasmonic devices can rapidly replace the semiconductor fabrication in communication technology due to high speed terahertz scale response and high energy electronic transport. Plasmon excitations are highly efficient in photovoltaic and catalytic designs for more effective solar energy harvesting by collective electron transport [75, 76]. Recent investigations confirm that nanoscale metallic compounds can be used to effectively convert collected electromagnetic energy at metal surfaces into high power electricity in local surface plasmon resonance (LSPR) mechanism via the so-called hot electron generation [77]. Plasmonic devices may operate at small wavelength $(10 - 380)$nm range in high precision engineering design with relatively higher cost. The generate energetic electrons can be collected in a tandem design with an appropriate electron accepting nanolayer such as, TiO_2 [78]. Due to vast applications, there has been an ongoing intense research towards exploration of plasmonic field in recent years [79–84].

One of the great advantages of plasmonic technology is the effective parametric control over the collective excitations instabilities by means of exceptional points technology. Due to both wave- and particle-like coupled oscillations of plasmons, a collisionless energy exchange among wave and the electrons is possible and may be used to manipulate the physical properties of the quantum plasmonic devices. The singular exceptional points are critical points around which the physical behavior of the system changes radically. Such points has been used in parametric control of the behavior of various coupled physical systems such as mechanical, optical, quantum, etc. [85]. In current research we show that the plasmonic system processes a full featured exceptional point phase structure which can have possible applications in plasmonic device fabrication. In this work we also introduce a new feasible photo-plasmonic mechanism for energetic electron tunneling trough the metal surface based on the exceptional points of the damped Schrödinger-Poisson system. The arrangement of the paper is as follows. We present the theoretical model in Sec. II. In Sec. III we describe the exceptional point structure of the lossless Hermitian system. The non-Hermitian system as a model for half-space plasmon excitation is described in Sec. IV. The photo-plasmonic process in collective electron tunneling is introduced in Sec. V and conclusion is presented in Sec. VI.

II. THE THEORETICAL MODEL

We consider electron gas of arbitrary degeneracy with neutralizing positive ionic background. The dynamics of the Madelung quantum electron fluid may be described using the following coupled effective Schrödinger-Poisson system [61] the well-known the

$$i\hbar\frac{\partial\mathcal{N}(\mathbf{r},t)}{\partial t} = -\frac{\hbar^2}{2m}\Delta\mathcal{N}(\mathbf{r},t) - e\phi(\mathbf{r})\mathcal{N}(\mathbf{r},t) + \mu\mathcal{N}(\mathbf{r},t), \tag{1a}$$

$$\Delta\phi(\mathbf{r}) = 4\pi e(|\mathcal{N}(\mathbf{r},t)|^2 - n_0), \tag{1b}$$

where $\mathcal{N}(\mathbf{r},t) = \psi(\mathbf{r},t)\exp[iS(\mathbf{r},t)/\hbar]$ is the statefunction characterizing the probability which is related to the fluid local electron number density $n(\mathbf{r}) = \psi(\mathbf{r},t)\psi^*(\mathbf{r},t)$ with n_0 being the uniform neutralizing background and the electron fluid momentum is given by $\mathbf{p}(\mathbf{r},\mathbf{t}) = \nabla S(\mathbf{r},t)$. The chemical potential μ is related to the local electron number density and the equilibrium temperature by appropriate isothermal equation of state (EoS) [64]. In the static limit $\mathbf{p} = 0$, one may Fourier analyse the appropriately linearized system around the equilibrium state $\{\psi^0 = 1, \phi^0 = 0, \mu^0 = \mu_0\}$ in scaled form [63] by assuming the plane-wave perturbations $\mathcal{N}(\mathbf{r},t) \propto \exp[i(\mathbf{k}\cdot\mathbf{r} - \epsilon t)]$ and $\phi(\mathbf{r}) \propto \exp[i(\mathbf{k}\cdot\mathbf{r})]$ in which the energy ϵ and wavenumber k are normalized, respectively to the plasmon energy $E_p = \sqrt{4\pi e^2 n_0/m}$ and $k_p = \sqrt{2mE_p}/\hbar$ to arrive at the energy dispersion of $E = k_w^2 + k_e^2$. Note that $E = (\epsilon - \mu_0)/E_p$ is the normalized energy and k_w and k_e characterizing the wave-like and particle-like oscillations, respectively. The dual wavenumber character of oscillations is an intrinsic feature of quantum fluid oscillations [64]. Moreover, the coupled wave-particle oscillations admit a complementarity-like relation $k_w k_e = 1$ in dimensionless form. The energy dispersion can be written in a more useful form of $E_k = k^2 + 1/k^2$ in which k is the characteristic wavenumber of collective electron excitations.

Using the standard quantum statistical definition, one may obtain thermodynamic quantities for collective excitations. Because there is a one-to-one correspondence between the single-electron and collective excitations energy levels [61], analogous to quantum liquid quasiparticle states, the Pauli exclusion principle also applies to collective modes. Starting with the number of quasiparticle modes we have $N_k = 4\pi k^3/3$ which leads to the density of states (DoS) $D_k = (dN_k/dk)/|dE_k/dk|$ with the quasiparticle occupation function of $F_k = 1/[1 + \exp(E_k/\theta)]$ in which $\theta = T/T_p$ being the normalized electron temperature to the plasmon temperature $T_p = E_p/k_B$. Some important quantities such as the normalized number-density $n(\theta)$, internal energy

$U(\theta)$ and heat capacity $c(\theta)$ are given as

$$n(\theta) = \int_0^\infty \frac{D_k dk}{1+\exp(E_k/\theta)}, \quad D_k = \frac{2\pi k^5}{|k^4-1|}, \tag{2a}$$

$$U(\theta) = \int_0^\infty \frac{D_k E_k dk}{1+\exp(E_k/\theta)}, \quad E_k = k^2 + \frac{1}{k^2}, \tag{2b}$$

$$c(\theta) = \frac{\partial}{\partial\theta} \int_0^\infty \frac{D_k E_k dk}{1+\exp(E_k/\theta)}, \tag{2c}$$

Figure 1 shows some thermodynamic properties of collective excitations (plasmon quasiparticles) in electron gas of arbitrary degeneracy. Figure 1(a) depicts the DoS as a function of quasiparticle wavenumber. A Van-Hove-like singularity is present for the plasmon wavenumber $k = k_p$ which is analogous to a similar singularity at the Fermi surface of crystalline solid [1]. it is remarked that DoS increases with increase of plasmon wavenumber almost linearly for large k values, similar to that of a free-electron gas [1]. The plasmon occupation function is shown in Fig. 1(b) for different values of normalized electron temperature. The plasmon occupation shows a distinct difference with that of free electron gas. It is remarked that occupation at the long wavelength limit is strongly prohibited for the collective modes as opposed to free electron case [1]. It is also shown that increase of the normalized electron temperature lead to overall increase in occupation probability of quasiparticles which is enhances at wavenumbers close to the plasmon wavenumber. In Fig. 1(c) we show the number of modes per wavenumber range, $D_k F_k(\theta)$. Largest modes in wavenumber range are localized around the plasmon wavenumber increase with increase in normalized temperature of electrons. However, this increase is seen to be more significant for $k > k_p$ rather than $k < k_p$. The normalized number-density, internal energy and heat capacity contribution from collective electron excitations as a function of the normalized electron temperature are shown in Fig. 1(d). It is remarked that number-density and internal energy of quasiparticles increase with increase of the normalized electron temperature, θ. Moreover, variation of quasiparticle heat capacity is reminiscent to that of free electron gas [1] excitations at low temperatures as compared to the Debye one. The only deference is that the low temperature contribution of collective excitations is missing due to the sharp decrease of collective modes at low temperature. It is concluded that while single electron excitation are more common at low temperature limit and cause saturation of heat capacity at high temperature limit, the quasiparticle excitation contribute mostly to high temperature heat capacity.

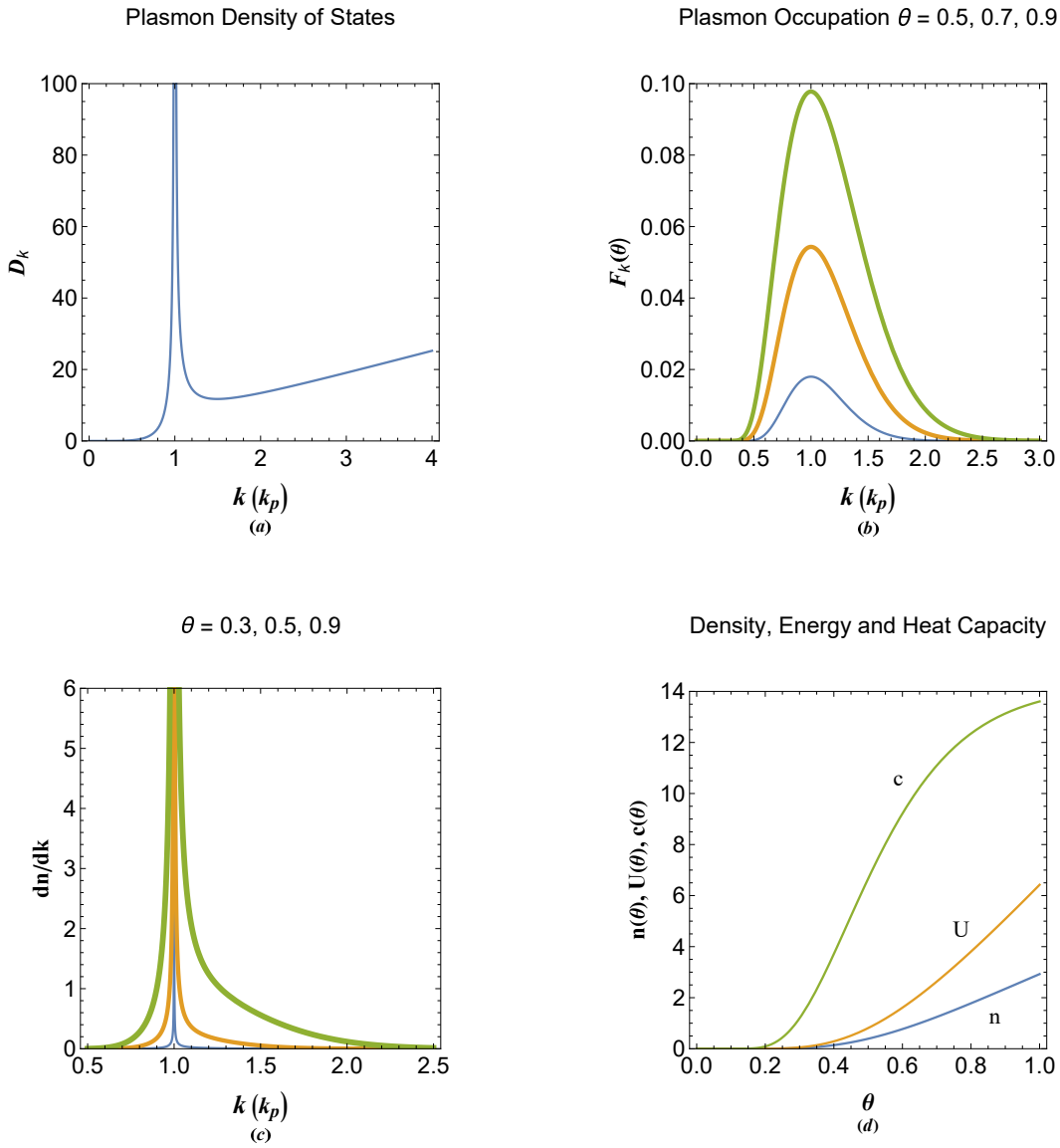

FIG. 1. (a) The normalized plasmon density of states (DoS) as a function plasmon wavenumber. (b) The normalized plasmon occupation function variation with the wavenumber for different normalized electron temperature. The increase in the curve thickness indicate the increase in the electron temperature. (c) The normalized plasmon mode in unit wavenumber for different electron temperature values. (d) The plasmon electron number-density, internal energy and heat capacity as a function of the normalized electron temperature.

III. PLASMON DISPERSION AND EXCEPTIONAL POINT STRUCTURE

The 3D linearized system obtained from (1) can be solved exactly in stationary radial form [65]. However, the one dimensional case has lot of applications which admits simple station-

ary analytic solution which is considered here. The normalized linear coupled system after separation of variables reads [64]

$$\frac{d^2\Psi(x)}{dx^2} + \Phi(x) + E\Psi(x) = 0, \tag{3a}$$

$$\frac{d^2\Phi(x)}{dx^2} - \Psi(x) = 0, \tag{3b}$$

where $\Psi(x)\Psi^*(x) = n(x)$ and $\Phi(x)$ denotes the local electrostatic potential energy. With the tentative boundary values $\Psi(0) = 1$ ans $\Phi(0) = \Psi'(0) = \Phi'(0) = 0$ we have the solution of the form

$$\Phi(x) = \frac{\cos(k_w x) - \cos(k_e x)}{\sqrt{\mathrm{E}^2 - 4}}, \tag{4a}$$

$$\Psi(x) = \frac{\left(\mathrm{E} + \sqrt{\mathrm{E}^2 - 4}\right)\cos(k_e x) - \left(\mathrm{E} - \sqrt{\mathrm{E}^2 - 4}\right)\cos(k_w x)}{2\sqrt{\mathrm{E}^2 - 4}}, \tag{4b}$$

where k_w and k_e are the coupled oscillations wave and particle wavenumbers

$$k_w = \sqrt{\frac{\mathrm{E} - \sqrt{\mathrm{E}^2 - 4}}{2}}, \quad k_e = \sqrt{\frac{\mathrm{E} + \sqrt{\mathrm{E}^2 - 4}}{2}}. \tag{5}$$

Note that $k_w k_e = 1$ holds as previously put forward.

Figures 2(a) and 2(b) depict the real and imaginary parts of the wavenumbers, respectively. The evident branching point at $E = 2$ is reminiscent of the exceptional point found in damped harmonic oscillator problem with applications in many physical instances a good review of wich may be found in Ref. [85]. However, occurrence of such feature in Hermitian systems like ours is quite interesting. Recently, it has been shown that such aspect is found in coupled oscillators with damping replaced by the elastic coupling [86]. Such a collisionless damping [87, 88] is a well-known feature of wave-particle interactions in electron plasmas. The existence of exception point in the coupled system (3) may be the mathematical manifestation of the kinetic Landau damping effect. note that the solution (4) does not apply to the exceptional (singular) point for which $k_w = k_e = k_p$ or equivalently $E = 2$. The solution at exceptional point is

$$\Phi(x) = \frac{x}{2}\sin(x), \quad \Psi(x) = \cos(x) - \frac{x}{2}\sin(x), \tag{6}$$

It is remarked that above the exceptional point both wavenumbers are real, wahereas, below this point theare complex with their real part the same but imaginary parts with opposite signs. This physically means wave-like(particle-like) spacial grow(decay) behavior of the collective excitations for $E < 2$.

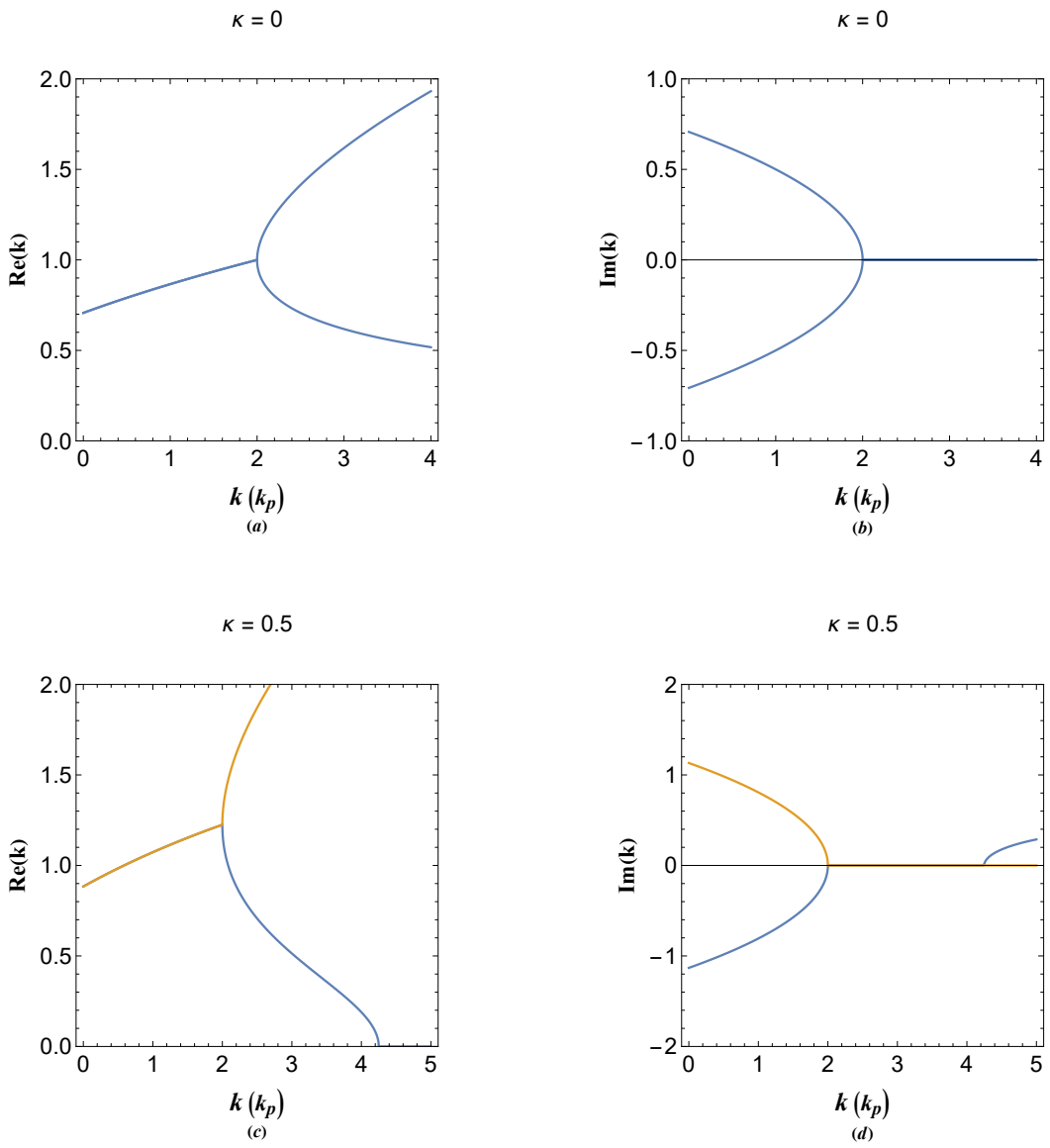

FIG. 2. Figs. (a) and (b), respectively, depict the real and imaginary parts of the energy dispersion of collective electron modes in the absence of damping effect. Figs. (c) and (d), respectively, depict the real and imaginary parts of the energy dispersion of collective electron modes in the presence of damping effect ($\kappa = 0.5$).

IV. THE PSEUDO-DAMPED PLASMON EXCITATIONS

Let us now consider the non-Hermitian system with damping effect

$$\frac{d^2\Psi(x)}{dx^2} + 2\kappa\frac{d\Psi(x)}{dx} + \Phi(x) + E\Psi(x) = 0, \tag{7a}$$

$$\frac{d^2\Phi(x)}{dx^2} + 2\kappa\frac{d\Phi(x)}{dx} - \Psi(x) = 0, \tag{7b}$$

in which κ is a new parameter characterizing the non-Hermiticity and can be used to model variety of physical situations [63, 64]. The system (7) has the following exact solution with the same boundary values $\Psi(0) = 1$ ans $\Phi(0) = \Psi'(0) = \Phi'(0) = 0$

$$\Phi(x) = \frac{\mathrm{e}^{-\kappa x}}{\sqrt{\mathrm{E}^2-4}}\left[\cos(k_w x) - \cos(k_e x) + \frac{\kappa}{k_w}\sin(k_w x) - \frac{\kappa}{k_e}\sin(k_p x)\right], \tag{8a}$$

$$\Psi(x) = \frac{\mathrm{e}^{-\kappa x}}{2\sqrt{\mathrm{E}^2-4}}\left[\left(\mathrm{E}+\sqrt{\mathrm{E}^2-4}\right)\cos(k_p x) - \left(\mathrm{E}-\sqrt{\mathrm{E}^2-4}\right)\cos(k_w x) + \right. \tag{8b}$$

$$\left.\frac{\kappa\left(\mathrm{E}+\sqrt{\mathrm{E}^2-4}\right)}{k_e}\sin(k_e x) - \frac{\kappa\left(\mathrm{E}-\sqrt{\mathrm{E}^2-4}\right)}{k_w}\sin(k_w x)\right], \tag{8c}$$

where the plasmon oscillation wavenumbers are given as

$$k_w = \sqrt{\frac{\mathrm{E}-2\kappa^2-\sqrt{\mathrm{E}^2-4}}{2}}, \quad k_e = \sqrt{\frac{\mathrm{E}-2\kappa^2+\sqrt{\mathrm{E}^2-4}}{2}}. \tag{9}$$

which satisfy the energy dispersion $E = (k^2+\kappa^2) + 1/(k^2+\kappa^2)$. Note that in the limit $\kappa = 0$ this reduces to the undamped plasmon dispersion. The existence of exponentially decaying term in the solution (7) causes the spacial damping of wavefunction and electrostatic potential energy for all orbital energy range. The real and imaginary parts of plasmon wavenumbers with damping parameter (κ) effect are shown in Figs. 2(c) and 2(d) for parameter value of $\kappa = 0.5$. It is clearly evident that a new exceptional point appears at $k \simeq 4.25$ in normalized unit beside the previous one at $k = 1$. Note that for energy values above the second exceptional point the wavenumber is purely particle-like. It is found that the new exceptional point is at $E = \kappa^2 + 1/\kappa^2$. It is noted that the energy dispersion relation of damped plasmon excitations only describes oscillation types and does not include the effect of exponentially decaying term on exceptional point structure. The later aspect of the solution (7) will be discussed in detail in the following section. The solution to the system (7) at the exceptional point $E = 2$ has the following form

$$\Phi(x) = \frac{\mathrm{e}^{-\kappa x}}{2(1-\kappa^2)^{3/2}}\left\{\left[\kappa - x\left(\kappa^2-1\right)\right]\sin\left(\sqrt{1-\kappa^2}x\right) - \kappa\sqrt{1-\kappa^2}x\cos\left(\sqrt{1-\kappa^2}x\right)\right\}, \tag{10a}$$

$$\Psi(x) = \frac{\mathrm{e}^{-\kappa x}}{2(1-\kappa^2)^{3/2}}\left[\left(\kappa^2 x + \kappa - 2\kappa^3 - x\right)\sin\left(\sqrt{1-\kappa^2}x\right) - \right. \tag{10b}$$

$$\left.\sqrt{1-\kappa^2}\left(2\kappa^2 - \kappa x - 2\right)\cos\left(\sqrt{1-\kappa^2}x\right)\right]. \tag{10c}$$

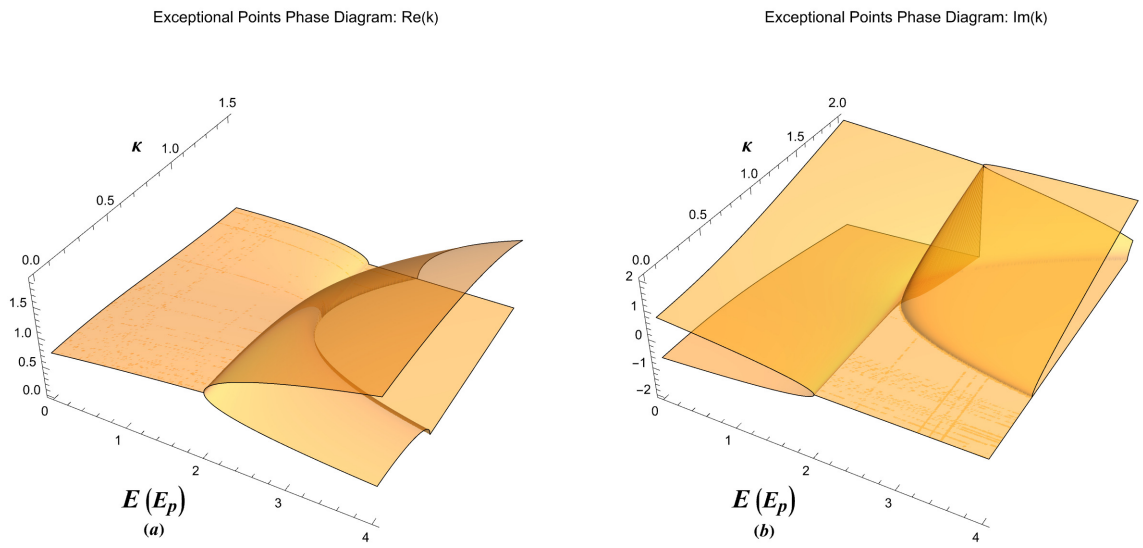

FIG. 3. The exceptional point phase diagram showing (a) the real part and (b) the imaginary part of the collective oscillation wavenumber in E-κ plane.

Furthermore, the solution at the exceptional point $E = \kappa^2 + 1/\kappa^2$ reads

$$\Phi(x) = \frac{\kappa^2 \mathrm{e}^{-\kappa x}}{\left(1-\kappa^4\right)^{3/2}} \left[(1+\kappa x)\sqrt{1-\kappa^4} - \sqrt{1-\kappa^4}\cos\left(\frac{\sqrt{1-\kappa^4}}{\kappa}x\right) - \kappa^2 \sin\left(\frac{\sqrt{1-\kappa^4}}{\kappa}x\right)\right], \tag{11a}$$

$$\Psi(x) = \frac{\mathrm{e}^{-\kappa x}}{\left(1-\kappa^4\right)^{3/2}} \left[\sqrt{1-\kappa^4}\cos\left(\frac{\sqrt{1-\kappa^4}}{\kappa}x\right) + \kappa^2 \sin\left(\frac{\sqrt{1-\kappa^4}}{\kappa}x\right) - \kappa^4 (1+\kappa x)\sqrt{1-\kappa^4}\right]. \tag{11b}$$

Figure 3 shows a full-featured 3D exceptional point phase-diagram in E-k plane. The real/imaginary part of wave-like and particle-like wavenumbers is shown in Fig. 3(a)/3(b). The exceptional points phase-diagrams in our case can have a wide variety of physical application such as in quantum charge screening, light scattering from metallic surfaces, etc. In the next section we will show an important application of the pseudodamping model in photoplasmonic effect. We also discuss different solutions and their physical interpretations in various regions of the phase diagram.

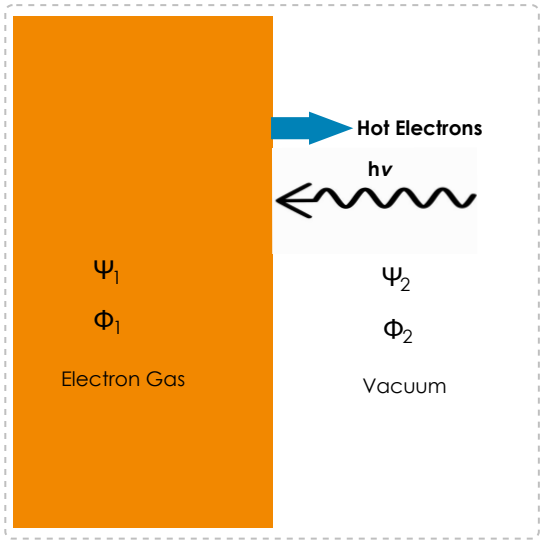

FIG. 4. The collective hot-electron generation at the metal-vacuum interface by incident energetic photo-plasmonic effect. The wavefunction $\Psi(x)$ and potential energy $\Phi(x)$ characterize the quantum state of each region.

V. THE HALF-SPACE EXCITATIONS AND PHOTO-PLASMONIC EFFECT

The model (7) has been recently used to describe the electron spill-out effect in half-space configuration where the parameter κ characterizes the collective electron tunneling parameter [63]. Figure 4 shows the schematic profile of the half-space plasmon excitations and photo-plasmonic effect in which the dashed region denotes the plasmonic material interfacing the vacuum. In reality the electron spill-out somehow blurs the interface causing an electron-ion separation and dipole formation. The incident high frequency photons have been shown to lead to collective extraction of hot electrons from the surface due to plasmon resonance. Here we provide an alternative clear physical description of hot electron mechanism in terms of the quantum electron tunneling effect. In the metallic region the collective excitations are stable above the exceptional point at $E = 2$. At thermal equilibrium, there are finite number of electrons excited to plasmon band as shown in Fig. 5(a). On the other hand, in the vacuum region the spill-out electrons form a narrow unstable plasmon band limited from above at $E = \kappa^2 + 1/\kappa^2$, as shown in Fig. 5(b). The variations of maximum energy of the plasmon band in vacuum in terms of electron tunneling parameter κ is depicted in Fig. 5(c) showing a minimum at $\kappa = 1$ where the two exceptional points coincide. Also, the plasmon ban minimum wavenumber varies with the parameter κ as see n in Fig. 5(d). Note that for $\kappa \geq 1$ there is

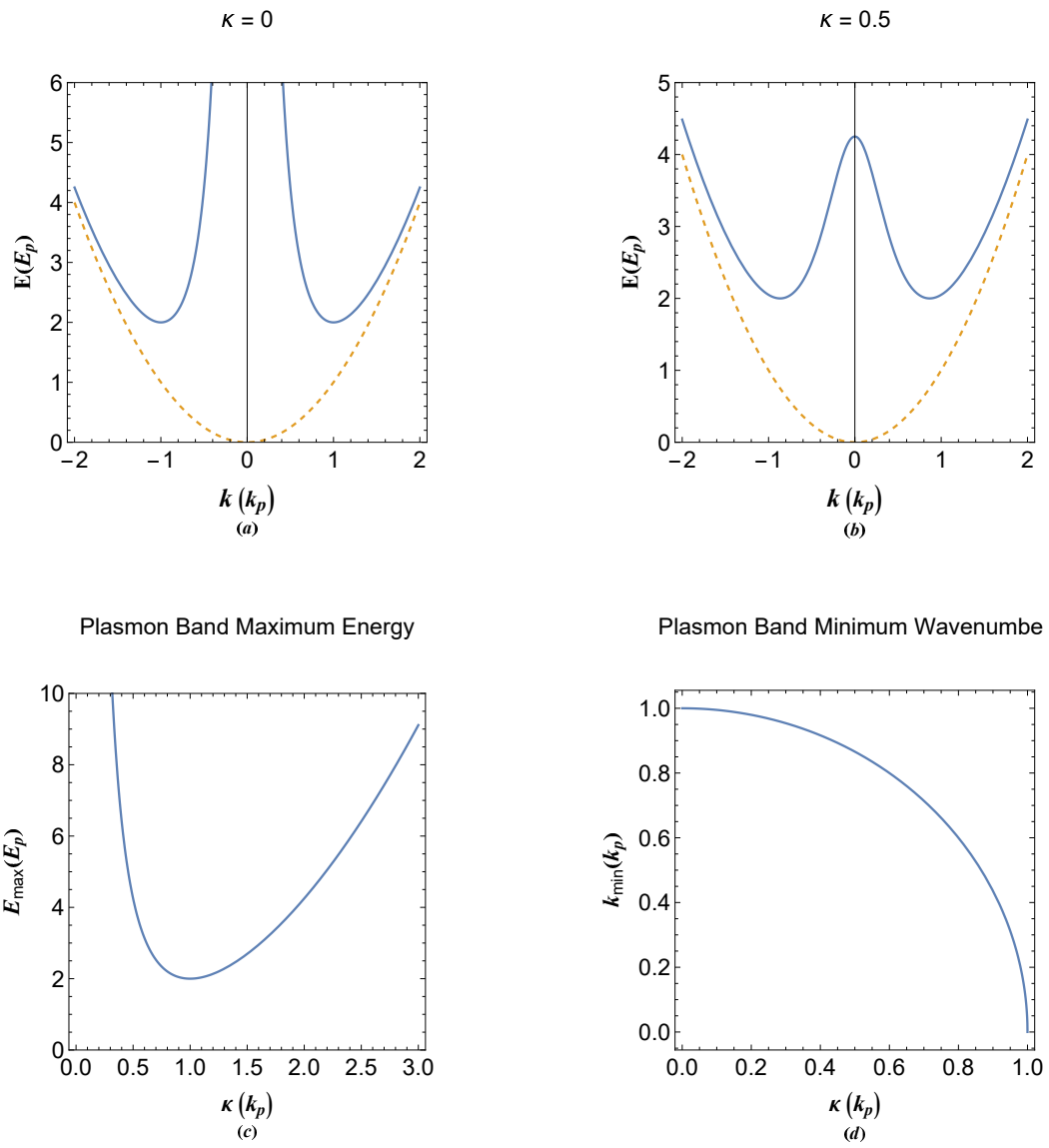

FIG. 5. (a) The energy dispersion of collective mode in metallic region without plasmon damping effect. (b) The energy dispersion f damped plasmon in the collective tunneling region (vacuum) for given value of the damping parameter ($\kappa = 0.5$). (c) The maximum energy in damped plasmon energy band of Fig. 5(b) as a function of the damping parameter. (d) The energy minimum wavenumber of damped plasmon conduction band as a function of the damping parameter. The dashed curves in plots (a) and (b) show the free electron dispersion.

onle a single exceptional point in the system.

Figure 6 depicts the excitation profiles in the metallic region below and above the exceptional energy value. Figure 6(a) shows the normalized wavefunction and electrostatic energy profiles at energy orbital $E = 2.3$ above the exceptional point. It is remarked that oscillations are

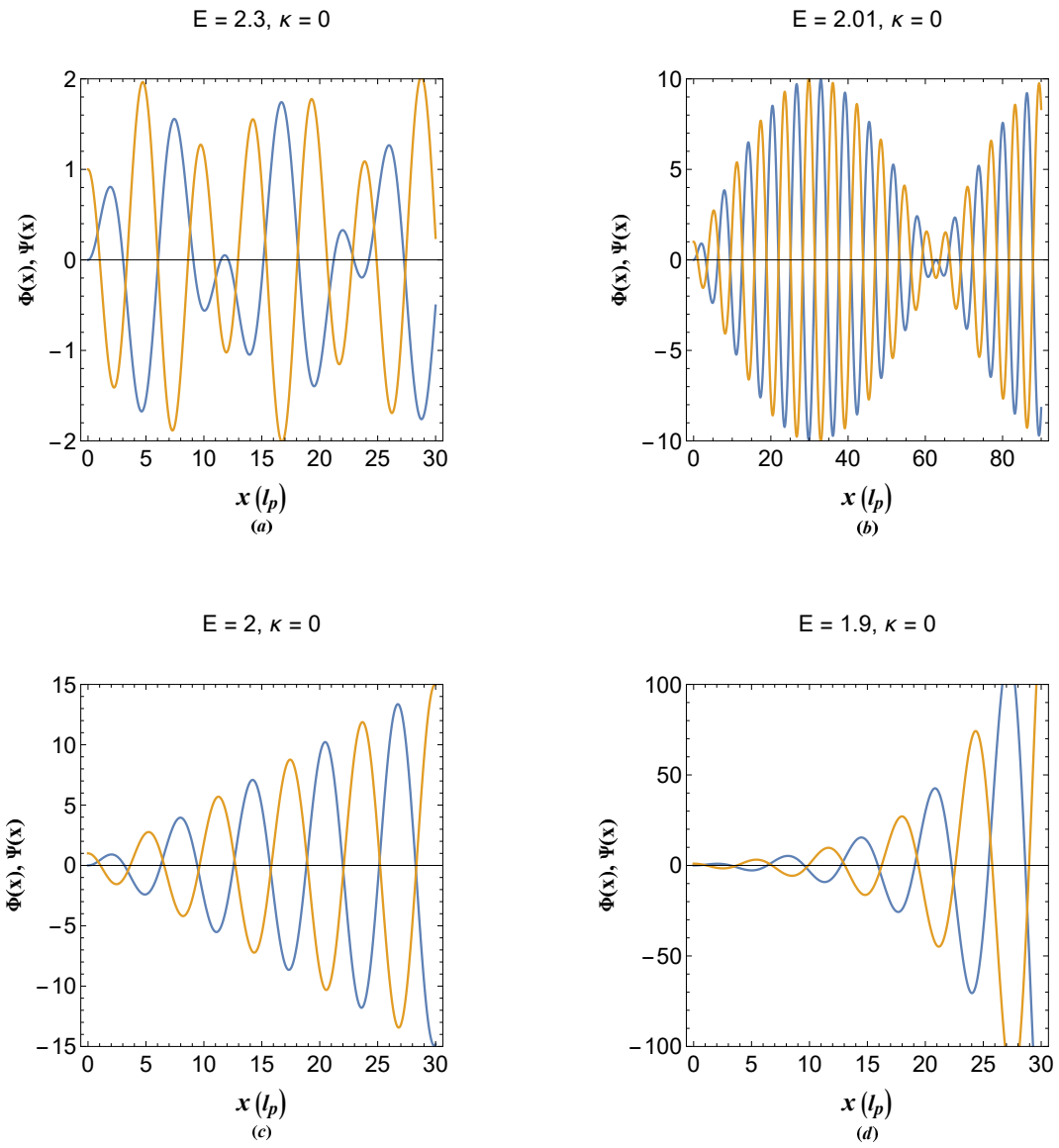

FIG. 6. (a) The collective oscillation profiles of the local wavefunction and electrostatic potential energy of undamped plasmons at overcritical energy orbital (orbitals above the exceptional point). (b) The collective oscillation profiles of the local wavefunction and electrostatic potential energy of undamped plasmons at nearcritical energy orbital (the quantum beating state). (c) The collective oscillation profiles of the local wavefunction and electrostatic potential energy of undamped plasmons at exceptional-point energy orbital (orbital at the exceptional point). (d) The collective oscillation profiles of the local wavefunction and electrostatic potential energy of undamped plasmons at under-critical energy orbital (orbitals below the exceptional point in plasmon energy gap region).

dual-tone due to wave-particle coupling and spatially stable. Moreover, Fig. 6(b) shows the profiles at orbital close to the exceptional point where $k_w \simeq k_e$, the so-called quantum beating region. At this point the electrons and the electrostatic potential energy tend to localize and the wave-particle interactions enhance. Figure 6(c) depict the solution at the exceptional point indicating that wavefunction and energy grows linearly, hence, the number density and energy oscillations are unstable. In face the region $0 < E < 2$ is a plasmon band gap in which no stable collective excitation can exist as also remarked in Fig. 6(d) for the gap energy orbital $E = 1.9$ with exponetial wave-like growth.

The excitations of tunneling (spill out) electrons in vacuum follow the solution (8). Figure 7 shows such excitations in different regions of parameters. Figure 7(a) shows the excitation profiles for energy orbital between the two exceptional points. It is seen that the oscillations strongly damp at distances far from the interface region due to the character of quantum electron tunneling. However, this damping is also double tone because of wave and particle excitations in this region. Figure 7(b) depicts the excitation profiles for orbital above the two exceptional point indicating that excitation are also damping in this region. Figures 7(c) and 7(d) show the excitation profiles at the exceptional point $E = 2$ and $E = \kappa^2 + 1/\kappa^2$, respectively. While the excitations at $E = 2$ are of nearly the same amplitude, at the other exceptional point amplitude of energy oscillations is much lower compared to that of the probability. It is also remarked that at exceptional points the oscillations are single tone due to coincidence of real and imaginary wavenumbers at such points.

Figures 8(a) and 8(b) show the excitation types in the plasmon band gap below the lowest exceptional point. It is shown that the excitations are of both decaying and growing type depending on orbital energy. However, both oscillation types in 8(a) and 8(b) are still unstable. It is found that there is exist a critical orbital in this region at which the excitations become stable. This is by no chance but due to the resonant matching of the tunneling (damping) parameter with the imaginary (growing) wave-like oscillation wavenumber. It is remarked that for each value of the tunneling parameter there is a distinct orbital, as it is termed the photo-plasmon orbital, E_{pp}, for which the excitation are not damped in vacuum. This is an important feature of plasmon excitations in damping environment which takes place solely due to dual character of collective electron excitations. The photo-plasmonic effect is the plasmon-assisted hot electron tunneling may be considered as the collective tunneling analogous of the well-know photo-electric effect. From Figs 8(c) and 8(d) it is remarked that while the wavenumber at the photo-plasmon orbital strongly varies with the change in value of the tunneling parameter, κ,

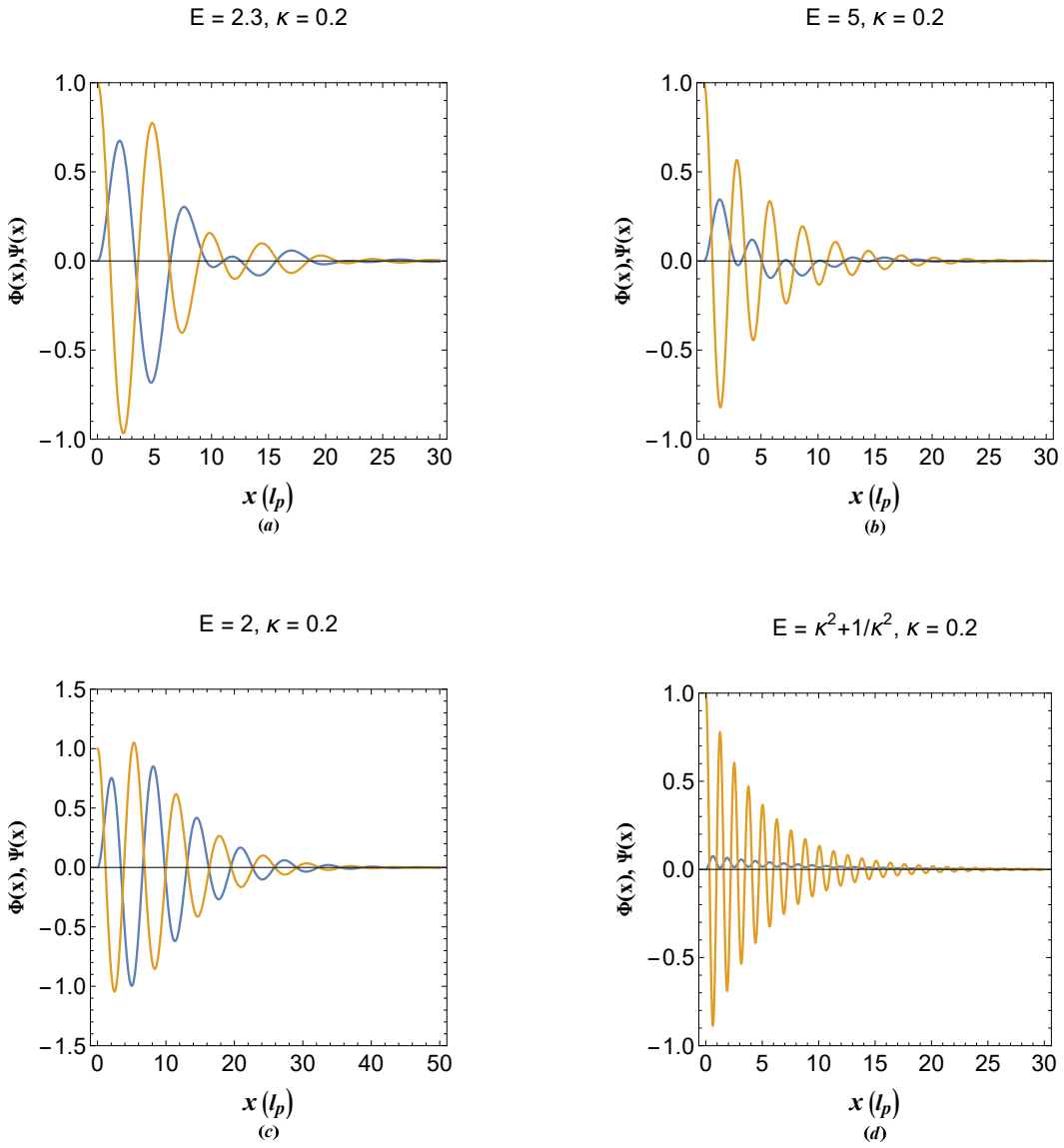

FIG. 7. (a) The collective oscillation profiles of the local wavefunction and electrostatic potential energy of damped plasmons at energy orbital between the two exceptionl points. (b) The collective oscillation profiles of the local wavefunction and electrostatic potential energy of damped plasmons at energy orbital above the two exceptional points. (c) The collective oscillation profiles of the local wavefunction and electrostatic potential energy of damped plasmons at exceptional-point energy orbital (orbital at the first exceptional point $E = 2$). (d) The collective oscillation profiles of the local wavefunction and electrostatic potential energy of damped plasmons at second exceptional-point energy orbital (orbital at the second exceptional point $E = \kappa^2 + 1/\kappa^2$).

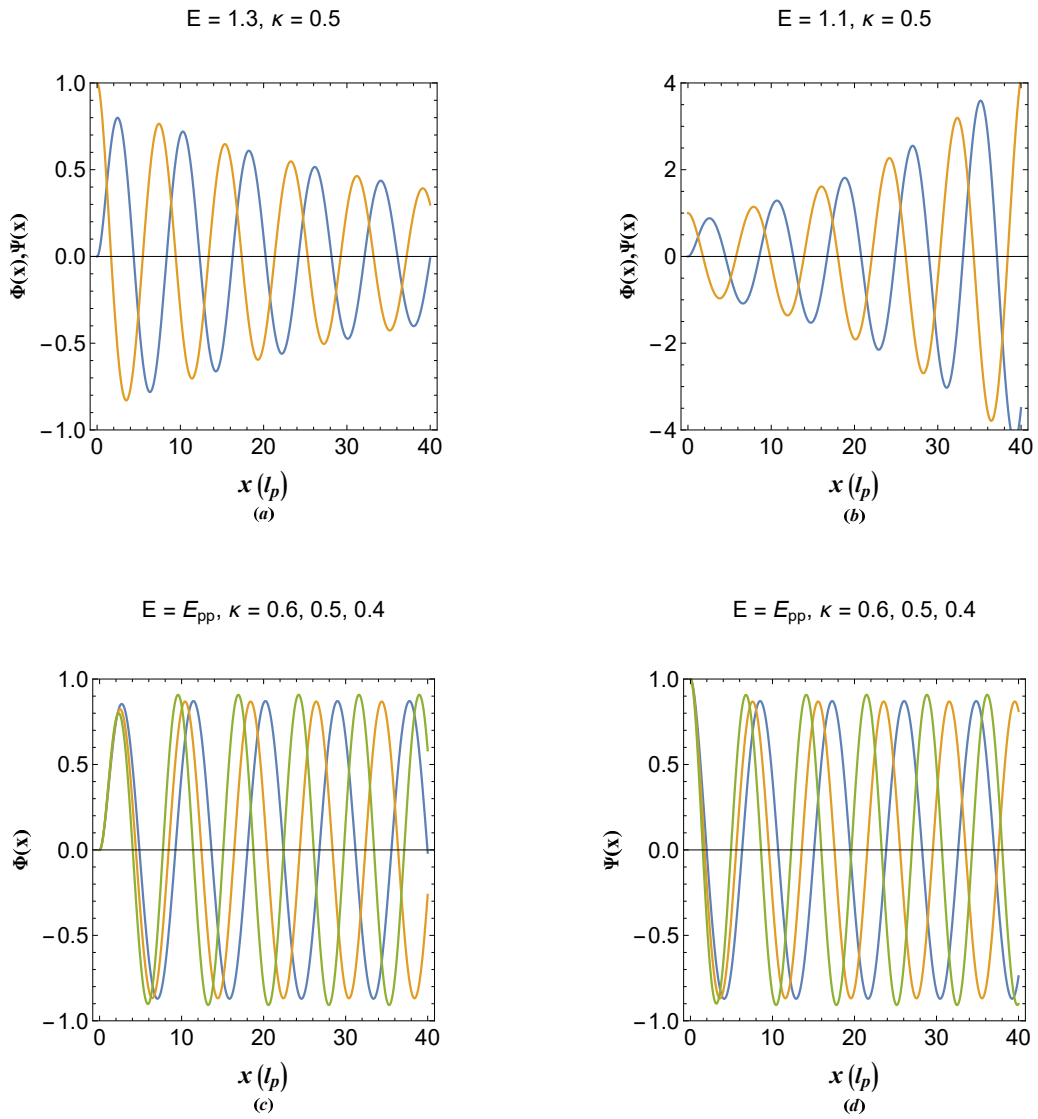

FIG. 8. (a) The decaying unstable collective oscillation profiles of the local wavefunction and electrostatic potential energy of dampes plasmons at energy orbital below the exceptionl point $E = 2$. (b) The growing unstable collective oscillation profiles of the local wavefunction and electrostatic potential energy of dampes plasmons at energy orbital below the exceptional point $E = 2$. (c) The stable collective oscillation profiles of the electrostatic potential energy of damped plasmons at resonant orbital below the exceptionl point $E = 2$. (d) The stable collective oscillation profiles of the wavefunction of damped plasmons at resonant orbital below the exceptionl point $E = 2$.

the amplitude of wavefunction and electrostatic energy of vacuum side is almost independent of this parameter. In reality energetic (hot) electrons can be excited to this photo-plasmonic orbital by radiation at the metallic surface and collectively tunnel through the vacuum potential

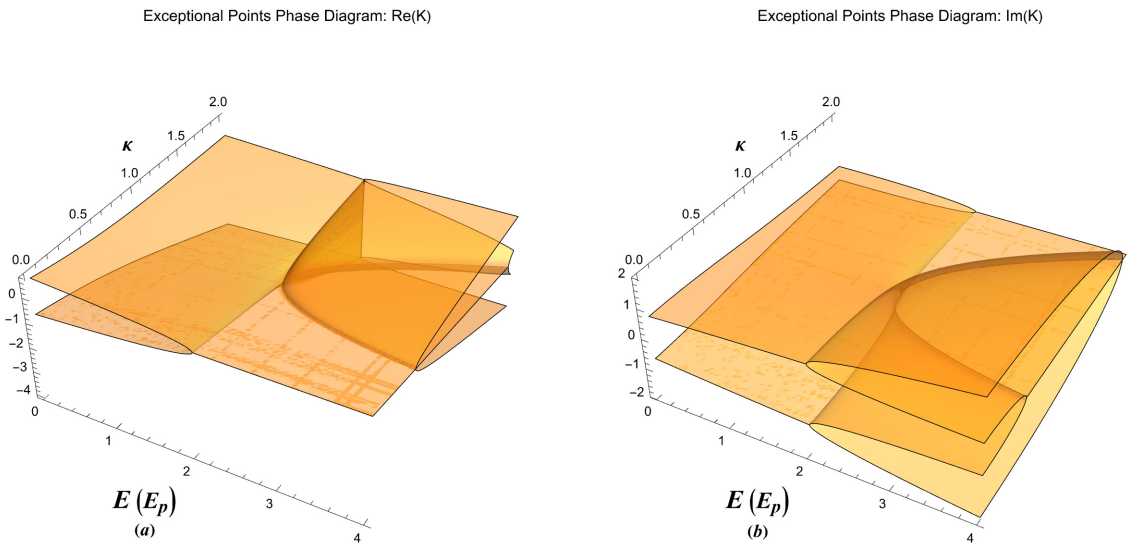

FIG. 9. (a) The real part of generalized damped plasmon wavenubers. (b) The imaginary part of generalized damped plasmon wavenubers.

barrier. This effect can have many applications in photo-plasmonic solar-cell designs for effective photo-electron energy extraction. Current solar cell designs rely on inefficient single electron-hole pair excitations at the Fermi level semiconductor junctions. The exact photo-plasmon energy eigenvalue E_{pp} is obtained from the following condition

$$\Im\left(\sqrt{\mathrm{E_{pp}} - 2\kappa^2 - \sqrt{\mathrm{E_{pp}}^2 - 4}}\right) + \sqrt{2}\kappa = 0, \tag{12}$$

where $\Im$ denotes the imaginary part of the complex variable. The generalized wavenumber of damped plasmon excitations (including the exponential damping term) may be written as

$$K_w^{\pm} = -\kappa \pm \mathrm{i}\sqrt{\frac{\mathrm{E} - 2\kappa^2 - \sqrt{\mathrm{E}^2 - 4}}{2}}, \quad K_e^{\pm} = -\kappa \pm \mathrm{i}\sqrt{\frac{\mathrm{E} - 2\kappa^2 + \sqrt{\mathrm{E}^2 - 4}}{2}}. \tag{13}$$

Therefore, the photo-plasmon tunneling condition is written as $\Re(K_w^+) = \Re(K_e^-) = 0$, where $\Re$ denotes the real part of a variable. It is also noted that the relation $\Im(K_w^{\pm}) = \Im(K_e^{\mp})$ always holds. The exceptional point phase diagram of the generalized wavenumber K is shown in Fig. 9. It is remarked that the structure of exceptional space in the plasmon tunneling region is much more complex as compared to that of Fig. 3. This makes possible to explore a variety of novel physical phenomenon with possible important technological applications of collective quantum electron tunneling and photo-plasmonic effect by fine tuning the photon energy and the tunneling parameter.

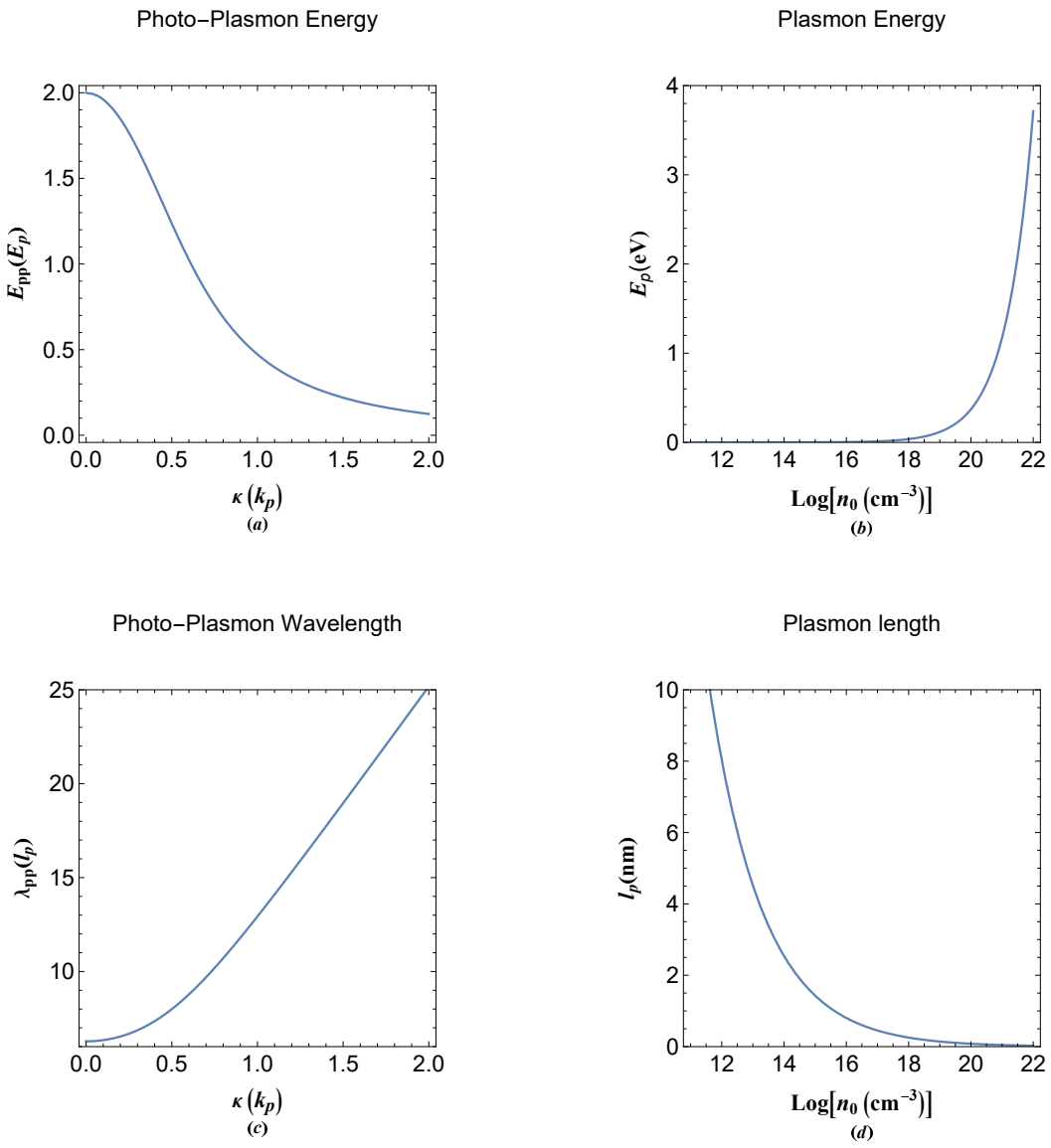

FIG. 10. (a) Variation of photo-plasmon energy with the pseudodamping parameter which is related to the collective tunneling coefficient in the plasmon parameter units. (b) The variation in plasmon energy unit with electron number-density. (c) The variation of photo-plasmon wavelength with resoect to the damping parameter. (d) variation of plasmon length in nanometer unit with the electron concentration.

In Fig. 9(a) we have shown the photo-plasmon energy variation with the pseudodamping parameter in plasmon parameter units. It is remarked that the photo-plasmon energy reduces by increase in the damping parameter which directly related to the metal-vacuum interface quantum electron tunneling phenomenon. The maximum energy is seen to correspond to the undamped case. Technically the hot-electron extraction may include some efficient tandem

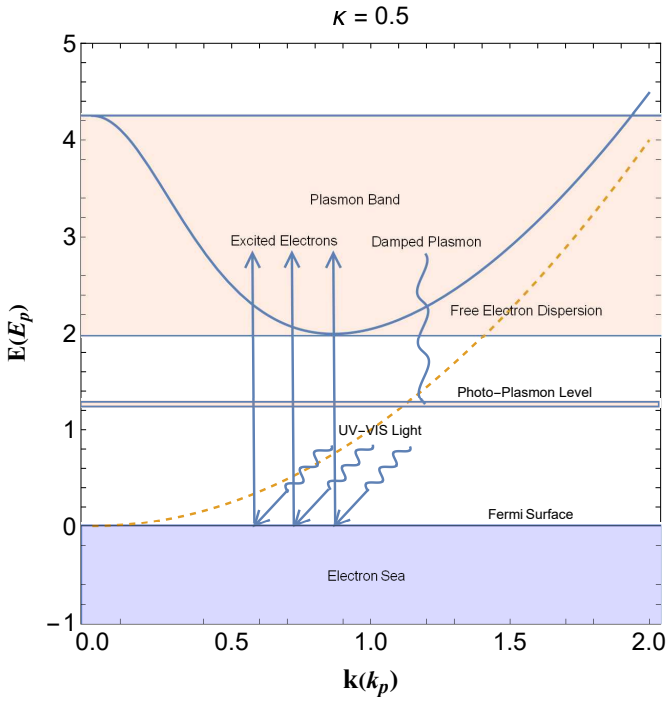

FIG. 11. Schematic of the photo-plamonic phenomenon in arbitrary degenerate electron gas. The dashed curve represents the free electron dispersion and the solid one denotes the damped plasmon dispersion.

multilayer material arrangements for best performance. To compare the energy scale in plasmonic devices we have shown the variation of the plasmon energy unit with the free electron concentration in Fig. 9(b). The values of this energy for typical metallic densities are few electronvolts. For the aluminium as one of goon plasmonic material candidate this energy can be high around $E_p^{Al} \simeq 15$eV. Figure 9(c) depicts the variation in the photo-plasmon wavelength in plasmon length ($l_p = 1/k_p$) units. It is clearly evident that by increase in the damping parameter the photo-plasmon wavelength increases sharply. The variation of plasmon length with electron number-density is shown in Fig. 9(d) in nanometers. For typical metals the photo-plasmon wavelength seems to be around few nanometers for reasonable value of the damping parameter.

Figure 11 shows the schematic of photo-plasmonic effect at the surface of plasmonic metal with $\kappa = 0.5$. The dashed curve depict the free electron dispersion and the solid curve denotes the damped plasmon energy dispersion. The point $E = 0$ denotes the Fermi energy level below which electrons are packed at zero temperature. It is remarked that electrons at the Fermi surface of the metal are excited to the plasmon band by energetic visible or ultraviolet

radiation. They collectively damp and fall into the photo-plasmon energy level from which they collectively tunnel through vacuum or semiconductor. Note that the collective excitation feature of damped plasmon is the main reason for the formation of the photo-plasmon level and consequent collective hot-electron tunneling. Also note that electrons excited beyond the depicted plasmon band lack the wave-like oscillations and do not contribute to the photo-plasmonic effect via plasmon damping. The plasmon band play the role of a collective stirring room for energetic electrons quite similar in nature to the starling murmuration phenomenon.

VI. CONCLUSION

In this research based on the effective damped Schrödinger-Poisson model we proposed a novel collective hot electron generation mechanism at metal-vacuum interfaces. We studied the exceptional behavior of collective excitations from the energy dispersion relation for both undamped and damped differential system revealing a full featured exceptional point phase diagram for plasmon excitations. Such exceptional behavior are of fundamental importance and technological applications in many branches of physical sciences. We showed that a similar mechanism as the photo-electric effect (so-called photo-plasmonic effect) exists for the collective excitations at the metal surfaces illuminated by appropriate radiations. The high energy photo-plasmonic electrons may be used in highly efficient plasmonic solar-cell devices for energy harvesting purposes. The photo-plasmonic effect is also physically important phenomenon in understanding collective electron tunneling and electron spill-out in metallic surfaces and metal-semiconductor interfaces.

VII. DATA AVAILABILITY

The data that support the findings of this study are available from the corresponding author upon reasonable request.

VIII. REFERENCES

[1] C. Kittel, Introduction to Solid State Physics, (John Wiely and Sons, New York, 1996), 7th ed.

[2] N. W. Ashcroft and N. D. Mermin, Solid State Physics (Saunders College Publishing, Orlando, 1976).

[3] K. Seeger, Semiconductor Physics (Springer, Berlin, 2004) 9th ed.

[4] C. Hu, Modern Semiconductor Devices for Integrated Circuits (Prentice Hall, Upper Saddle River, New Jersey, 2010) 1st ed.

[5] H. A. Atwater, The Promise of Plasmonics, Sci. Am. **296**, 56(2007); doi.org/10.1038/scientificamerican0407-56

[6] G. Manfredi, Preface to Special Topic: Plasmonics and solid state plasmas, Phys. Plasmas **25**, 031701(2018); https://doi.org/10.1063/1.5026653

[7] S. A. Maier, Plasmonics: Fundamentals and Aplications, Springer Science Business Media LLC (2007).

[8] H. Haug and S. W. Koch, "Quantum theory of the optical and electronic properties of semiconductors", World Scientific, 2004,

[9] P. A. Markovich, C.A. Ringhofer, and C. Schmeister, Semiconductor Equations (Springer, Berlin, 1990).

[10] A. D. Yofee, Low-dimensional systems: quantum size effects and electronic properties of semiconductor microcrystallites (zero-dimensional systems) and some quasi-two-dimensional systems, Adv. Phys., **42**, 173-262(1993), DOI: 10.1080/00018739300101484

[11] Alexander L. Fetter, Phys, Rev. B, **32** 7676 (1985).

[12] G. D. Mahan, Many-particle physics, 2nd edition, chapter 5 (Plenum press, New York, 1990).

[13] Feynman, Richard, QED: The Strange Theory of Light and Matter. Princeton University Press (1985).

[14] W. Kohn, L. J. Sham, "Self-Consistent Equations Including Exchange and Correlation Effects". Physical Review. **140** (4A) 1133 (1965); doi:10.1103/PhysRev.140.A1133

[15] C. Gardner, The quantum hydrodynamic model for semiconductor devices, SIAM, J. Appl. Math. **54** 409(1994).

[16] S. Ichimaru, Strongly coupled plasmas: high-density classical plasmas and degenerate electron liquids, Rev. Mod. Phys. **54**, 1017 (1982); doi.org/10.1103/RevModPhys.54.1017

[17] S. Ichimaru, H. Iyetomi, and S. Tanaka, Statistical physics of dense plasmas: Thermodynamics, transport coefficients and dynamic correlations, Phys. Rep. **149**, 91 (1987); doi.org/10.1016/0370-1573(87)90125-6

[18] S. Ichimaru, *Statistical Physics: Condensed Plasmas* (Addison Wesely, New York, 1994).

[19] G. Manfredi, "How to model quantum plasmas," Fields Inst. Commun. **46**, 263–287 (2005); in Proceedings of the Workshop on Kinetic Theory (The Fields Institute, Toronto, Canada 2004): http://arxiv.org/abs/quant–ph/0505004.

[20] F. Haas, *Quantum Plasmas: An Hydrodynamic Approach* (Springer, New York, 2011).

[21] Zh. A. Moldabekov, M. Bonitz, and T. S. Ramazanov, Phys. Plasmas **25**, 031903 (2018); https://doi.org/10.1063/1.5003910

[22] E. Fermi and E. Teller, Phys. Rev. **72**, 399 (1947).

[23] D. Bohm and D. Pines, Phys. Rev. **92** 609(1953).

[24] Bohm, D. Phys. Rev. **85**, 166–179 (1952).

[25] Bohm, D. Phys. Rev. **85**, 180–193 (1952).

[26] D. Pines, Phys. Rev. **92** 609(1953).

[27] P. Levine and O. V. Roos, Phys. Rev, **125** 207(1962).

[28] Y. Klimontovich and V. P. Silin, in Plasma Physics, edited by J. E. Drummond (McGraw-Hill, New York, 1961).

[29] T. Takabayasi, Prog. Theor. Phys., **8** 143(1952).

[30] T. Takabayasi, Prog. Theor. Phys., **14** 283(1955).

[31] T. Takabayasi and J. P. Vigier, Prog. Theor. Phys., **18** 573(1957).

[32] T. Takabayasi, Prog. Theor. Phys., **9** 187(1953).

[33] T. Takabayasi, Nuovo Cim, **7** 118(1958).

[34] C. Castro and J. Mahencha, Prog. Phys., **1** 38(2006).

[35] C. Castro, J. Math. Phys., **31** 2633(1990).

[36] C. Castro, Found. Phys. Lett., **4** 81(1991).

[37] C. Castro, Found. Phys., **4** 569(1992).

[38] J. Lindhard, Dan. Mat. Fys. Medd. 28(8), 1 (1954),

[39] M. Marklund and G. Brodin, Dynamics of Spin-1/2 Quantum Plasmas, Phys. Rev. Lett. **98**, 025001(2007); doi.org/10.1103/PhysRevLett.98.025001

[40] M. Bonitz, D. Semkat, A. Filinov, V. Golubnychyi, D. Kremp, D. O. Gericke, M. S. Murillo, V. Filinov, V. Fortov, W. Hoyer, J. Phys. A, **36** 5921(2003).

[41] P. K. Shukla, B. Eliasson, "Nonlinear aspects of quantum plasma physics" Phys. Usp. **53** 76(2010)

[42] L. Stenflo, G. Brodin, J. Phys. Plasmas, **76** 261(2010).

[43] M. Akbari-Moghanjoughi, Phys. Plasmas **22**, 022103 (2015); *ibid.* **22**, 039904 (E) (2015).

[44] P. K. Shukla and B. Eliasson, Phys. Rev. Lett. **99**, 096401(2007).

[45] L Stenflo Phys. Scr. **T50** 15(1994).

[46] P. K. Shukla, B. Eliasson, and L. Stenflo Phys. Rev. E **86**, 016403(2012).

[47] G. Brodin and M. Marklund, New J. Phys. **9**, 277(2007).

[48] M. Marklund and G. Brodin, Phys. Rev. Lett. **98**, 025001(2007).

[49] N. Crouseilles, P. A. Hervieux, and G. Manfredi, Phys. Rev. B **78**, 155412 (2008).

[50] Z. Moldabekov, Tim Schoof, Patrick Ludwig, Michael Bonitz, and Tlekkabul Ramazanov, Phys. Plasmas, **22**, 102104(2015); doi.org/10.1063/1.4932051

[51] Hwa-Min Kim and Young-Dae Jung, EPL, **79** 25001(2007).

[52] F. Haas, G. Manfredi, P. K. Shukla, and P.-A. Hervieux, Phys. Rev. B, **80**, 073301 (2009).

[53] E. Madelung, Z. Phys., 40 322(1926).

[54] H. R. Miller, P. J. Witta, Active Galetic Nuclei, Springer-Verlag, Berlin, (1987) pp. 202.

[55] P. Goldreich, W. H. Julian, Astrophys. J., **157** 869(1969).

[56] F. C. Michel, Rev. Mod. Phys., **54** 1(1982).

[57] E. Tandberg-Hansen, A.G. Emshie, The Physics of Solar Flares, Cambridge Univ. Press, Cambridge,(1988) pp.124.

[58] M. J. Rees, in: G. B. Gibbons, S. W. Hawking, S. Siklas (Eds.), The Very Early Universe, Cambridge Univ. Press, Cambridge, (1983).

[59] W. Misner, K.S. Throne, J.A. Wheeler, Gravitation, Freeman, San Francisco, (1973) pp.763.

[60] M. Akbari-Moghanjoughi, Sci. Rep. **11**, 21099 (2021).

[61] M. Akbari-Moghanjoughi, Phys. Plasmas, **26**, 012104 (2019); doi.org/10.1063/1.5078740

[62] M. Akbari-Moghanjoughi, Phys. Plasmas, **26**, 072106 (2019); doi.org/10.1063/1.5097144

[63] M. Akbari-Moghanjoughi, Physics of Plasmas **29**, 082112 (2022); doi.org/10.1063/5.0102151

[64] M. Akbari-Moghanjoughi, Phys. Plasmas, **26**, 112102 (2019); https://doi.org/10.1063/1.5123621

[65] M. Akbari-Moghanjoughi, Phys. Plasmas, **26**, 062105 (2019); doi.org/10.1063/1.5090366

[66] L. Stanton and M. S. Murillo, Phys. Rev. E **91**, 033104(2015).

[67] J. Hurst, K. L. Simon, P. A. Hervieux, G. Manfredi and F. Haas, Phys. Rev. B **93**, 205402(2016).

[68] B. Eliasson and P. K. Shukla, Phys. Scr. **78**, 025503 (2008).

[69] M. I. Stockman, Nanoplasmonics: past, present, and glimpse into future. Opt Express **19** 22029 (2011).

[70] D. K. Gramotnev, S. I. Bozhevolnyi, Plasmonics beyond the diffraction limit. Nat Photonics **4** 83 (2010).

[71] Z. Zhou, E. Sakr, Y. Sun, P. Bermel, Solar thermophotovoltaics: reshaping the solar spectrum. Nanophotonics **5** 1 (2016).

[72] I. Goykhman, B. Desiatov, J. Khurgin, J. Shappir, U. Levy, Locally oxidized silicon surface-plasmon Schottky detector for telecom regime. Nano Lett **11** 2219 (2011).

[73] C. Haffner, D. Chelladurai, Y. Fedoryshyn, et al., Low-loss plasmon-assisted electro-optic modulator. Nature **556** 483 (2018).

[74] S. Ummethala, T. Harter, K. Koehnle, et al., THz-to-optical conversion in wireless communications using an ultra-broadband plasmonic modulator, Nat. Photonics **13**, 519(2019); doi.org/10.1038/s41566-019-0475-6

[75] C. Calvero, Plasmon-induced hot-electron generation at nanoparticle/metal-oxide interfaces for photovoltaic and photocatalytic devices, Nat. Photonic **8**, 95(2014); doi.org/10.1038/nphoton.2013.238

[76] Jacob B. Khurgin, Fundamental limits of hot carrier injection from metal in nanoplasmonics, Nanophotonics **9(2)**, 453(2020); doi.org/10.1515/nanoph-2019-0396

[77] H. A. Atwater and A. Polman, Plasmonics for improved photovoltaic devices, Nat. Mater. **9**, 205(2010); DOI: 10.1038/nmat2629

[78] Y. Tian and T. Tatsuma, Mechanisms and Applications of Plasmon-Induced Charge Separation at TiO2 Films Loaded with Gold Nanoparticles, J. Am. Chem. Soc. **127**, 7632(2005); doi.org/10.1021/ja042192u

[79] Jianing Chen, Michela Badioli, Pablo Alonso-González, Sukosin Thongrattanasiri, Florian Huth, Johann Osmond, Marko Spasenović, Alba Centeno, Amaia Pesquera, Philippe Godignon, Amaia Zurutuza Elorza, Nicolas Camara, F. Javier García de Abajo, Rainer Hillenbrand, Frank H. L. Koppens, Optical nano-imaging of gate-tunable graphene plasmons, Nat. **487** 77(2012); doi.org/10.1038/nature11254

[80] Z. Fei, A. S. Rodin, G. O. Andreev, W. Bao, A. S. McLeod, M. Wagner, L. M. Zhang, Z. Zhao, M. Thiemens, G. Dominguez, M. M. Fogler, A. H. Castro Neto, C. N. Lau, F. Keilmann, D. N. Basov, Gate-tuning of graphene plasmons revealed by infrared nano-imaging, Nat. **487** 82(2012); doi:10.1038/nature11253

[81] Hugen Yan, Tony Low, Wenjuan Zhu, Yanqing Wu, Marcus Freitag, Xuesong Li, Francisco Guinea, Phaedon Avouris, Fengnian Xia, Damping pathways of mid-infrared plasmons in graphene nanostructures, Nat. Photonics **7** 394(2013); doi:10.1038/nphoton.2013.57

[82] Xijiao Mu and Mengtao Sun, Interfacial charge transfer exciton enhanced by plasmon in 2D in-plane lateral and van der Waals heterostructures, Appl. Phys. Lett. **117**, 091601 (2020); doi.org/10.1063/5.0018854

[83] Rui Yang, Yuqing Cheng and Mengtao Sun, Aluminum plasmon-enhanced deep ultraviolet fluorescence resonance energy transfer in h-BN/graphene heterostructure, Optics Comm. **498**, 127224 (2021); doi.org/10.1016/j.optcom.2021.127224

[84] Jianuo Fan, Jizhe Song, Yuqing Cheng and Mengtao Sun, Pressure-dependent interfacial charge transfer excitons in WSe2-MoSe2 heterostructures in near infrared region, Results in Physics **24**, 104110 (2021); doi.org/10.1016/j.rinp.2021.104110

[85] Mohammad-Ali Miri and Andrea Alù, Science 363, 42 (2019).

[86] Carl E. Mungan and Trevor C, Lipscombe, Eur. J. Phys. **39** 025004 (2018).

[87] F. F. Chen, Introduction to Plasma Physics and Controlled Fusion, 2nd ed. (Plenum Press, New York, London, 1984).

[88] N. A. Krall and A. W. Trivelpeice, "Principles of Plasma Physics", (San francisco Press, San francisco 1986).